Title

A cyclic peptide antenna ligand for enhancing terbium luminescence

Journal

Analyst, 146(11)

ISSN

0003-2654

Authors

Ji, Fei
Shao, Shiqun
Li, Zhonghan
et al.

Publication Date

2021-06-07

DOI

10.1039/d1an00530h

Peer reviewed

HHS Public Access

Author manuscript

Analyst. Author manuscript; available in PMC 2022 June 07.

Published in final edited form as:

Analyst. 2021 June 07; 146(11): 3474–3481. doi:10.1039/d1an00530h.

A cyclic peptide antenna ligand for enhancing terbium luminescence

Fei Ji[#a], **Shiqun Shao**[#a], **Zhonghan Li**[a], **Siwen Wang**[a], **Rohit Chaudhuri**[a], **Zhili Guo**[a], **Nicole G. Perkins**[a], **Priyanka Sarkar**[a], **Min Xue**[a]

[a]Department of Chemistry, University of California, Riverside, Riverside, California 92521, United States

[#] These authors contributed equally to this work.

Abstract

We present here a cyclic peptide ligand, cy(WQETR), that binds to terbium ion (Tb^{3+}) and enhances Tb^{3+} luminescence intensity through the antenna effect. This peptide was identified through screening a cyclic peptide library against Tb^{3+} with an apparent EC_{50} of 540 μM. The tryptophan residue from the peptide directly interacts with the Tb^{3+} ion, which provides access to a low-lying triplet excited state of the tryptophan. Direct excitation of this triplet state enables energy transfer to the Tb^{3+} ion and enhances Tb^{3+} luminescence intensity by 150 fold. We further showcase the application of this cy(WQETR)-Tb^{3+} system by demonstrating the detection of tromethamine with a detection limit of 0.5 mM.

Keywords

Cyclic peptide; Terbium; Luminescence enhancement; Antenna effect

Introduction

As a luminophore, Tb^{3+} ion has many unique and outstanding features: the luminescence peaks are narrow, the intensities are stable, the Stokes shifts are large, the emission wavelengths are insensitive to the environment, and most importantly, the luminescence lifetime is long.[1, 2] However, there is one detrimental problem with Tb^{3+} ion - it has very small extinction coefficients in the UV region. For instance, $TbCl_3$ has molar extinction coefficients of 320 $M^{-1}cm^{-1}$ at 220 nm and 1.8 $M^{-1}cm^{-1}$ at 260 nm in water.[3] Consequently, direct excitation of Tb^{3+} ions is difficult and yields very weak luminescence.

As a strategy to overcome the weak absorption, a “photo antenna” design is often implemented.[1] In this scenario, an aromatic group absorbs a photon and transfers its excited state energy to a nearby Tb^{3+} cation. This energy transfer can take the format of a long-

Conflicts of interest

There are no conflicts to declare.

Electronic Supplementary Information (ESI) available: [details of any supplementary information available should be included here]. See DOI: 10.1039/x0xx00000x

range nonradiative transfer or a short-range Dexter exchange mechanism. This process causes the excitation of the Tb^{3+} cation and leads to luminescence. Because the selected aromatic groups have much higher extinction coefficients and absorb photons much more efficiently, the luminescence intensities are strongly enhanced.

There are two types of antenna design strategies. In the chromophoric chelate configuration, the antenna group contains coordinating atoms that directly bind to the Tb^{3+} cation. A representative example is the bipyridyl cryptand-based structures that were developed by Lehn and co-workers.[4] The other design is the pendant chromophore strategy, where the antenna group is not directly bound to the Tb^{3+} cation. A prominent example here is the carbostyril antenna on a diethylenetriaminepentaacetic acid scaffold developed by Selvin and co-workers.[5] Both strategies have proven effective and have enabled various types of Tb-based bioanalytical methods.[6–10] A particularly successful application is the homogenous time-resolved fluorescence assays,[11–13] where the long luminescence lifetime of the Tb^{3+} ions allows facile suppression of the background, especially the interference from intrinsic fluorophores in complex biological samples.

Despite their superior performance and commercial availability, Tb-based assays are not widely used as organic fluorophore-based ones. A limiting factor here is the cost. High-performance antenna ligands, such as the 2-hydroxyisophthalamide (IAM)-based ones developed by Raymond and co-workers,[1, 14] are relatively expensive and challenging to synthesize. Therefore, there has been a constant need for new antenna ligands. Nevertheless, creating antenna structures is not a trivial task. Most of the studies focus on modifying existing ligand scaffolds in the hope of improvements. Indeed, such exercises have yielded a panel of novel antenna ligands, but they all root from very limited chemical space.[1, 6, 15–19] On the other hand, *de novo* identification of antenna ligands is often incidental and difficult to predict, as demonstrated by the IAM antenna's discovery process.[1] Therefore, there is a pressing need to address the lack of new antenna ligands through a more systematic approach, such as high-throughput screening campaigns.

Inspired by the recent advances in peptide library screening technologies and successful examples of cyclic peptide-based affinity probes,[20–23] we hypothesized that we could identify new antenna ligand scaffolds through performing cyclic peptide library screening against Tb^{3+}. The rationale that motivated us contained five aspects. First, Tb^{3+} was known to bind to some proteins,[24–26] especially metalloproteins, through interacting with carboxyl and hydroxyl residues. Second, such binding could often lead to enhanced Tb^{3+} luminescence, which was due to the exclusion of solvent molecules as well as antenna effects from tryptophan and tyrosine residues. Third, the conformational constraints could enable cyclic peptides to mimic the metal-binding sites in metalloproteins. Fourth, many types of cyclic peptides were able to bind with metal ions and enable bioanalytical applications.[23] Fifth, Tb-binding sequences have been identified through residue-targeted screening approaches based on metal-binding linear peptides.[27, 28]

Herein, we report a cyclic peptide sequence, cy(WQETR), identified through a library screening campaign against Tb^{3+} ions. We show that this peptide can bind to Tb^{3+} and enhance Tb^{3+} luminescence through antenna effects. We further demonstrate that this

peptide can enable the detection of tromethamine in complex biological systems such as serum-containing cell culture media.

Results and Discussion

Cyclic peptide library screening identifies ligands that enhance Tb^{3+} luminescence

We chose a one-bead-one-compound monocyclic peptide library containing five modular amino acid residues as our model system.[20] This library was used by other groups and us to generate affinity probes for challenging protein epitopes.[20, 29] To construct the library, we first prepared a linear peptide library according to well-established split-pool protocols.[29] We then cyclized the peptides through a copper(I)-catalyzed azide-alkyne cycloaddition reaction. The fully assembled library contained approximately 1.8 million unique sequences, which established a large chemical space.

The screening process was described in Fig. 1A. We first removed sequences with high non-specific binding properties by pre-clearing the library.[29] Subsequently, we incubated the library with 20 μM of $TbCl_3$ in Tris buffer (10 mM, pH 7.4). After incubation and washing, we illuminated the beads with a hand-held UV lamp to identify potential hits. Indeed, we found ~20 beads that were luminescent brightly with a pale green hue – the signature of Tb^{3+} luminescence. These beads were picked out from the library, and their sequences were identified through established mass spectrometry-based methods.[29]

To validate the hit sequences, we synthesized those cyclic peptides in milligram quantities and tested if they were able to enhance Tb^{3+} luminescence. As shown in Fig. 1B, eight sequences showed enhanced luminescence compared with $TbCl_3$. This enhancement was homogeneous across the signature Tb^{3+} emission bands at 490 nm ($^5D_4$-$^7F_6$), 545 nm ($^5D_4$-$^7F_5$), 588 nm($^5D_4$-$^7F_4$), and 620 nm ($^5D_4$-$^7F_3$). Among the sequences, cy(WQETR) exhibited the highest enhancement – the resulting luminescence intensity was 150 times of that from $TbCl_3$ alone. Fig. 1C showed a comparison of Tb^{3+} solution and Tb^{3+} incubated with cy(WQETR) excited using a hand-held UV lamp, in which the cy(WQETR) greatly enhanced the luminescence intensity. Based on this result, we chose cy(WQETR) as the best candidate and used it to perform all subsequent studies. The peptide of cy(WQETR) was purified using RP-HPLC (Fig. S1) and validated with MALDI-TOF MS (Fig. S2).

cy(WQETR) binds to Tb^{3+}

We sought to validate if cy(WQETR) was indeed binding to Tb^{3+}. To test the proposed binding, we incubated $TbCl_3$ with varying concentrations of cy(WQETR) solutions and measured the resulting luminescence intensities. As shown in Fig. 2A, while the Tb^{3+} concentration was kept constant, increasing cy(WQETR) concentrations led to growing luminescence intensities. Because the data points followed a sigmoidal growth trend, we were able to fit them using a Hill function. Such a nonlinear response curve supported our theory that there was binding between cy(WQETR) and Tb^{3+}, and the apparent EC_{50} was determined to be 540 μM.

To further validate the observed binding and to refute the alternative hypothesis that the enhanced luminescence was due to altered ionic strength in the solution, we performed

isothermal titration calorimetry experiments. Here, we titrated a solution of $TbCl_3$ with a solution of cy(WQETR) and measured the resulting heat change. As shown in Fig. 2B, the generated isotherms exhibited a biphasic structure. The first few injections led to increasingly negative enthalpy changes, and after the 1.0 cy(WQETR)/Tb^{3+} molar ratio, further increasing the peptide concentration caused an obvious positive trend. This result proved that there were binding events during the titration course. We identified multiple binding sites (Fig. 2C) through data fitting, which were consistent with results generated from similar metal-protein binding experiments.[30]

The tryptophan residue in cy(WQETR) directly interacts with the Tb^{3+} ion

To better understand the binding between cy(WQETR) and Tb^{3+}, we studied this interaction's photophysical properties. We first checked if the tryptophan residue was involved in the Tb^{3+} coordination, which would dictate whether the potential antenna ligand belonged to the chromophoric chelate or pendant chromophore configuration.[1] As shown in Fig. 3A, cy(WQETR) displayed an absorption band around 280 nm, a tryptophan residue signature.[31] Upon adding Tb^{3+}, this tryptophan band showed a hyperchromic shift with a 10% increase of absorption. This change was indicative of the direct interaction between the tryptophan group and the Tb^{3+} ion. On the other hand, the absorption peaks' positions did not change, and the overall peak shape also remained the same. Based on these observations, we inferred that the tryptophan residue was likely interacting with the Tb^{3+} through a cation-π mechanism.[32] Therefore, if the tryptophan residue was serving as an antenna, it would be categorized as a chromophoric ligand.

It is also worth pointing out that a prominent tail emerged in the UV-vis spectrum at wavelengths immediately higher than the expected tryptophan absorption band. This new absorption peak was interesting because it hinted at the existence of a transition from the singlet ground state to a low-lying excited state of tryptophan.[24, 33, 34] Most likely, a transition to a triplet state was promoted as the result of the tryptophan-Tb^{3+} interaction. This result also supported our theory that the tryptophan residue was directly interacting with the Tb^{3+} ion.

We then examined if the Tb^{3+} binding affected the tryptophan fluorescence. If the tryptophan residue directly interacted with the Tb^{3+} ion, the corresponding tryptophan fluorescence intensity would decrease because such an interaction would promote additional nonradiative relaxation pathways from the singlet excited state of tryptophan. In addition, because the UV spectra hinted at additional low-lying excited states (Fig. 3A), we also expected an increased intersystem crossing efficiency, which would lead to decreased tryptophan fluorescence. Indeed, we observed that the addition of Tb^{3+} ions caused the tryptophan fluorescence intensity to decrease by 5% (Fig. 3B). This result further proved that the tryptophan residue in cy(WQETR) directly interacted with the Tb^{3+} ion.

Besides the tryptophan residue that directly interacted with the Tb^{3+} ion, the glutamic acid and threonine residues should also interact with Tb^{3+} through the hydroxyl group. The glutamine residue could also bind with Tb^{3+} through the side-chain amide group. The arginine residue was less likely to bind because of its positive charge in buffer. Nevertheless,

the arginine residue might help with solubilizing the ligand and assist the binding through promoting a privileged conformation.

cy(WQETR) enhances Tb^{3+} luminescence through tryptophan-based antenna effects

It is well-known that polydentate ligands that bind to Tb^{3+} could enhance Tb^{3+} luminescence by excluding solvent molecules, i.e., water, from the coordination sphere.[1, 35, 36] This repelling effect prevents water molecules from quenching the Tb^{3+} excited state, thereby increasing the luminescence quantum yield. However, such an interaction does not solve the lack of photon absorption and therefore has limited enhancing abilities. The greatly enhanced luminescence intensity resulting from cy(WQETR) hinted against the simple coordination effect and pointed to antenna effects. Moreover, tryptophan groups are proven antennas in the Tb-protein binding scenarios. Therefore, we hypothesized that cy(WQETR) enhanced Tb^{3+} luminescence through antenna effects.

To validate the antenna effect, we obtained the excitation profile of the cy(WQETR)-Tb system by scanning different excitation wavelengths and recording the corresponding luminescence intensity at 545 nm as the readout. The result is shown in Fig. 4A. There was an obvious peak in the excitation profile, which pointed to the existence of a prominent energy transfer-based antenna effect that led to the enhanced Tb^{3+} luminescence. Nevertheless, we needed to validate that this peak was indeed an energy transfer rather than a unique coupling of states specific to the Tb^{3+} $^5D_4$-$^7F_5$ transition. We obtained the excitation profiles corresponding to the other emission bands at 490 nm, 588 nm, and 620 nm, and we found the same excitation peaks in all of them (Fig. 4B). Taken together, these results proved the existence of the antenna effect.

Interestingly, the excitation profiles did not overlap with the tryptophan absorption peak at 280 nm. Instead, the excitation peak maximum was at 308 nm. This result contained rich information about the photophysical processes manifested in the antenna effect. As solid evidence, it proved that tryptophan's singlet excited state did not directly transfer energy to Tb^{3+}. This result was consistent with the common mechanism of antenna effects: the energy transfer usually originates from the antenna's triplet excited state rather than its singlet state.[24, 37, 38] Similarly, the lack of an excitation peak at 280 nm also proved that the intersystem crossing between the singlet and triplet excited states of tryptophan was of low efficiency and that this intersystem crossing was incapable of contributing significantly to the antenna effect. More importantly, the excitation peak at 308 nm seemed to overlap well with the newly emerged absorption band between 300–340 nm. This overlap indicated a direct excitation from the tryptophan ground state to its low-lying triplet excited state, and a subsequent energy transfer to Tb^{3+} led to luminescence. Such a process was consistent with tryptophan's known photophysical properties: multiple low-lying triplet excited states exist,[33, 34] and a direct transition from the ground state to the triplet excited states is possible.[34]

cy(WQETR) does not saturate the Tb^{3+} coordination sphere

As mentioned above, ligand binding to Tb^{3+} can prevent solvent molecule-induced luminescence quenching.[35] Therefore, it is beneficial to occupy all the coordination sites of Tb^{3+}. To test if cy(WQETR) was able to saturate the Tb^{3+} coordination sphere, we tested

how different buffer solutions affected the cy(WQETR)-Tb luminescence. As shown in Fig. 5, HEPES buffer led to the highest luminescence intensity, followed by Tris (tromethamine hydrochloride) and sodium acetate. This result proved that cy(WQETR) did not occupy all the Tb^{3+} coordination sites and that there were water molecules in the coordination sphere. Because Tb^{3+} has a high affinity towards oxygen atoms,[1, 2] it was not surprising that oxygen-containing species (HEPES, tromethamine, and acetate) were able to replace water molecules and enhance the luminescence. As expected, ammonium chloride had minimal interaction with Tb^{3+} and did not enhance the luminescence.

cy(WQETR)-Tb^{3+} as a luminescence sensor for tromethamine

Inspired by the results above (Fig. 5), we envisioned that the cy(WQETR)-Tb^{3+} system could serve as a sensor for auxiliary ligands such as tromethamine. We tested how different concentrations of tromethamine affected cy(WQETR)-Tb^{3+} luminescence, and we found that increasing tromethamine concentrations led to consistently growing luminescence intensities, with a detection limit of 0.5 mM (Fig. 6A). This trend proved that we could analyze tromethamine concentration using cy(WQETR)-Tb^{3+} as a sensor. We then tested if such a relationship would survive in complex biological samples. We performed similar experiments in cell culture media, with and without fetal bovine serum. As shown in Fig. 6B, the trends were well-retained in these systems, albeit with increased detection limits (~30 mM). This result further validated the potential of using the cy(WQETR)-Tb^{3+} system to quantify tromethamine. Furthermore, it demonstrated the stability of the cy(WQETR)-Tb^{3+} interaction in complex biological samples.

Experimental

Chemicals and reagents

TentaGel S-NH_2 resin (0.28 mmol/g) was purchased from Rapp Polymere GmbH (Tübingen, Germany). Rink amide MBHA resin (0.678 mmol/g) was purchased from Aapptec (Louisville, KY). Fmoc-protected amino acids otherwise indicated were purchased from Anaspec. Fmoc-L-propargylglycine (Pra) and Fmoc-L-azidolysine (Az4) were purchased from Combi-Blocks (San Diego, CA). Piperidine was purchased from Alfa Aesar (Ward Hill, MA). Trifluoroacetic acid (TFA) and Hexafluorophosphate azabenzotriazole tetramethyl uronium (HATU) were purchased from Oakwood Chemical (Estill, SC). Diisopropylethylamine (DIEA), Cyanogen bromide (CNBr), and Terbium (III) chloride hexahydrate were purchased from Acros Organics (Fair Lawn, NJ). Triisopropylsilane (TIPS) and phenyl isothiocyanate (PhNCS) were purchased from TCI (Portland, OR). Cuprous iodide (CuI), Penicillin-Streptomycin (PS), and α-cyano-4-hydroxycinnamic acid (CHCA) were bought from Sigma-Aldrich (St. Louis, MO). N,N-dimethylformamide (DMF), acetonitrile, ethyl acetate (EA), diethyl ether (Et_2O), dichloromethane (DCM), ammonium chloride, hydrochloric acid, HEPES, and L-ascorbic acid were purchased from Thermo Fisher Scientific (Waltham, MA). Sodium acetate was purchased from Macron Fine Chemicals (Radnor Township, PA). 1X Dulbecco's Modified Eagle Medium (DMEM) and Fetal Bovine Serum (FBS) were purchased from Corning Cellgro. Tris hydrochloride was purchased from MP Biomedicals (Solon, OH). All the chemicals were used as received.

Synthetic procedures

Solid-phase peptide synthesis.—Peptides were synthesized on Rink Amide MBHA resin via the standard Fmoc SPPS method either manually or with the CSBio CS336S peptide synthesizer (Menlo Park, CA). Briefly, to connect an amino acid to the resin, the Fmoc group on the resin was removed by 20% piperidine/DMF solution (10 min, three times). The resin was then washed and drained with DMF for 5 times. Fmoc-AA-OH (3 equiv.), DIEA (5 equiv.), and HATU (2.8 equiv.) were mixed in DMF for 10 min. The mixture was then introduced to the deprotected resin and gently agitated for 1 h at room temperature. Afterwards, the resin was washed with DMF for five times and ready for the next amino acid. For click cyclized peptides, the cyclization was performed through a copper(I)-catalyzed azide-alkyne cycloaddition reaction. Specifically, resins were agitated in 20% Lutidine/DMF with CuI (2.5 equiv.) and L-ascorbic acid (5 equiv.) at room temperature overnight. After cyclization, the resins were washed with 5% w/v sodium diethyldithiocarbamate and 5% v/v DIEA in DMF to remove copper. The deprotection and cleavage of the peptides were performed in a TFA cleavage solution (TFA:TIPS:ddH_2O; 95:2.5:2.5) gently stirred for 2 h at room temperature. The crude peptides were purified through the RP-HPLC (DIONEX Ultimate 3000; Thermo Scientific, Idstein, Germany) with a C18 reversed-phase preparative column (Kinetex® 5 μm EVO, 250 × 21.2 mm). The final product's mass was confirmed with MALDI-TOF MS (AB SCIEX TOF/TOF 5800; Framingham, MA).

One-bead-one-compound (OBOC) cyclic peptide library construction.—A randomized one-bead-one-compound library of cyclic peptides was synthesized with split-and-pool strategy on TentaGel S-NH_2 resins. Az4 and Pra were introduced at the C-terminal and N-terminal, respectively. Eighteen natural amino acids (except Methionine and Cysteine) were used as building blocks at five randomized positions. The library was then cyclized and deprotected with the methods described previously. Afterwards, the deprotected resins were washed with DMF, methanol, and DMF, and stored under Argon for further use.

OBOC library screening.—The library was precleared following the established procedures.[29] Then 500 mg of resin from the library was swelled in tris buffer for 2 h and then incubated with 20 μM of $TbCl_3$ in tris buffer for 6 h. After incubation and washing, the beads were illuminated with a hand-held UV lamp. All luminescent hits were picked out; washed with water, DMF, and DCM; and dried under vacuum for the following sequencing.

Sequencing of the hits.

Edman degradation.: The Edman degradation was performed with the method adapted from the literature.[29] The hit beads were transferred to a glass vial with 50 μL of 2.5% PhNCS in pyridine/water (1:1). The vial was flushed with N_2 for 10 s, sealed with a stopper and then put in a water bath at 50 °C for 30 min. Afterwards, the solution was removed, and the beads were washed three times with ethyl acetate and once with DCM. Then the beads were air-dried and mixed with 100 μL of TFA, flushed with N_2 for 10 s, sealed with a stopper and then incubated in a water bath at 50 °C for 10 min. The solution was then diluted with 200 μL of ethyl acetate and removed. Afterwards, the beads were washed with

ethyl acetate twice and DCM once. Then the beads were incubated with a 20% TFA/water solution at 60 °C for 20 min, washed with ethyl acetate and DCM, and then air-dried.

Cleavage of the peptides from single beads.: After the Edman degradation, each individual hit bead was transferred to a microcentrifuge tube with 10 μL of water. Then 10 μL of CNBr (0.5 M in 0.2 N HCl solution) was added. The vessel was purged with argon and placed in a microwave oven for 1 min. Afterwards, the solution was dried with a centrifugal vacuum chamber at 45 °C for 2 h.

Sequencing by MALDI-TOF MS/MS.: 0.55 μL of CHCA solution (4 mg/mL in v/v 1:1 ACN/H_2O containing 0.1 % TFA) was added in each microcentrifuge tube. The mixture was spotted onto a MALDI plate and air-dried. Then the sample was analyzed by MALDI-TOF to obtain the MS/MS spectra. The spectra were analyzed to determine the sequences.[29]

Luminescence measurement.—$TbCl_3$ was incubated with various hits of cyclic peptides in 0.1 M of Tris buffer. The final concentration of Tb^{3+} is 0.5 mM, while the concentration of peptides was 5 mM. Then, 65 μL of the mixed solution was added into a Greiner black 384-well plate and incubated for 30 min. The luminescence intensity was measured using a Synergy H1 microplate reader with time-resolved mode. The delay time was set to be 75 μs and the data collection time was 1 ms. For different solvents, 0.1 M of Tris, NH_4Cl, and NaOAc, and 0.02 M of HEPES were used at pH 7.4. For cell culture media, DMEM and 10% fetal bovine serum were used.

Photophysical characterizations.—The UV-vis absorption of cy(WQETR) and cy(WQETR)-Tb^{3+} mixture was measured using Cary 5000 UV-vis-NIR spectrophotometer. The fluorescence intensity of tryptophan was measured using Horiba PTI QM-400 Fluorescence spectrophotometer.

Isothermal Titration Calorimetry (ITC) analysis.—The ITC analysis of cy(WQETR) and Tb^{3+} was performed on a MicroCal iTC200. In particular, the Tb^{3+} solution was placed in the sample cell, and 0.5 mM of cy(WQETR) was loaded into a syringe. A series of small aliquots were injected into the sample solution with a 180 s interval between each injection. Heat changes were measured, and the data were analyzed with MicroCal ITC-Origin analysis software and fitted with a two sequential-binding sites model.

Conclusions

In conclusion, we have identified a cyclic peptide ligand, cy(WQETR), that could bind to Tb^{3+} and enhance Tb^{3+} luminescence via an antenna effect. The tryptophan residue interacted with Tb^{3+}, which provided access to a low-lying triplet excited state. This triplet excited state could directly rise from the tryptophan ground state, and it could transfer energy to the Tb^{3+} ion, leading to enhanced Tb^{3+} luminescence. We further demonstrated that this cy(WQETR)-Tb^{3+} interaction could be utilized for analyzing tromethamine in cell culture media, even in the presence of serum.

Our results also demonstrated the feasibility of *de novo* discovery of antenna ligands through a library screening approach. Performing screening campaigns using more complex peptide libraries could yield additional ligand structures. Moreover, incorporating unnatural amino acid modules, especially those with appropriate triplet excited states, promises even better antenna groups.

Supplementary Material

Refer to Web version on PubMed Central for supplementary material.

Acknowledgements

We thank Prof. Christopher Bardeen and Prof. Gregory Beran for the helpful discussions. We gratefully acknowledge the financial support from grants 5R21EB025393 and 1R35GM138214 from the US National Institutes of Health.

References

1. Moore EG, Samuel APS and Raymond KN, Acc. Chem. Res, 2009, 42, 542–552. [PubMed: 19323456]
2. Richardson FS, Chem. Rev, 1982, 82, 541–552.
3. Onstott EI and Brown CJ, Anal. Chem, 1958, 30, 172–174.
4. Alpha B, Lehn J-M and Mathis G, Angew. Chem. Int. Ed, 1987, 26, 266–267.
5. Ge P and Selvin PR, Bioconj. Chem, 2004, 15, 1088–1094.
6. Bui AT, Grichine A, Duperray A, Lidon P, Riobé F, Andraud C and Maury O, J. Am. Chem. Soc, 2017, 139, 7693–7696. [PubMed: 28551987]
7. Falcone E, Gonzalez P, Lorusso L, Sénèque O, Faller P and Raibaut L, Chem. Commun, 2020, 56, 4797–4800.
8. Ocaña JA, Callejón M and Barragán FJ, Analyst, 2000, 125, 1851–1854. [PubMed: 11070553]
9. Hildebrandt N, Wegner KD and Algar WR, Coord. Chem. Rev, 2014, 273–274, 125–138.
10. Levoye A, Zwier JM, Jaracz-Ros A, Klipfel L, Cottet M, Maurel D, Bdioui S, Balabanian K, Prézeau L, Trinquet E, Durroux T and Bachelerie F, Front. Endocrinol, 2015, 6.
11. Degorce F, Card A, Soh S, Trinquet E, Knapik GP and Xie B, Curr. Chem. Genom, 2009, 3, 22–32.
12. Riddle SM, Vedvik KL, Hanson GT and Vogel KW, Anal. Biochem, 2006, 356, 108–116. [PubMed: 16797477]
13. Hemmilä I and Laitala V, J. Fluoresc, 2005, 15, 529–542. [PubMed: 16167211]
14. Petoud S, Cohen SM, Bünzli J-CG and Raymond KN, J. Am. Chem. Soc, 2003, 125, 13324–13325. [PubMed: 14583005]
15. Kawa M and Takahagi T, Chem. Mater, 2004, 16, 2282–2286.
16. Bui AT, Roux A, Grichine A, Duperray A, Andraud C and Maury O, Chem. Eur. J, 2018, 24, 3408–3412. [PubMed: 29341302]
17. Samuel APS, Xu J and Raymond KN, Inorg. Chem, 2009, 48, 687–698. [PubMed: 19138147]
18. Liu D, Zhou Y-N, Zhao J, Xu Y, Shen J and Wu M, J. Mater. Chem. C, 2017, 5, 11620–11630.
19. Li Y, Jiang ZW, Xiao SY, Huang CZ and Li YF, Anal. Chem, 2018, 90, 12191–12197. [PubMed: 30232881]
20. Agnew HD, Coppock MB, Idso MN, Lai BT, Liang J, McCarthy-Torrens AM, Warren CM and Heath JR, Chem. Rev, 2019, 119, 9950–9970. [PubMed: 30838853]
21. Sohrabi C, Foster A and Tavassoli A, Nat. Rev. Chem, 2020, 4, 90–101.
22. Buckton LK, Rahimi MN and McAlpine SR, Chem. Eur. J, 2021, 27, 1487–1513. [PubMed: 32875673]
23. Gahan LR and Cusack RM, Polyhedron, 2018, 153, 1–23.

24. Schlyer BD, Steel DG and Gafni A, J. Biol. Chem, 1995, 270, 22890–22894. [PubMed: 7559424]
25. Brittain HG, Richardson FS and Martin RB, J. Am. Chem. Soc, 1976, 98, 8255–8260. [PubMed: 993525]
26. Walters JD and Johnson JD, J. Biol. Chem, 1990, 265, 4223–4226. [PubMed: 2106517]
27. MacManus JP, Hogue CW, Marsden BJ, Sikorska M and Szabo AG, J. Biol. Chem, 1990, 265, 10358–10366. [PubMed: 2355005]
28. Nitz M, Franz KJ, Maglathlin RL and Imperiali B, ChemBioChem, 2003, 4, 272–276. [PubMed: 12672106]
29. Sarkar P, Li Z, Ren W, Wang S, Shao S, Sun J, Ren X, Perkins NG, Guo Z, Chang C-EA, Song J and Xue M, J. Med. Chem, 2020, 63, 6979–6990. [PubMed: 32491863]
30. Wilcox DE, Inorg. Chim. Acta, 2008, 361, 857–867.
31. Mach H, Middaugh CR and Lewis RV, Anal. Biochem, 1992, 200, 74–80. [PubMed: 1595904]
32. Isaac M, Denisov SA, Roux A, Imbert D, Jonusauskas G, McClenaghan ND and Sénèque O, Angew. Chem. Int. Ed, 2015, 54, 11453–11456.
33. Ghiron C, Bazin M and Santus R, J. Biochem. Bioph. Methods, 1988, 15, 337–348.
34. Tsentalovich YP, Snytnikova OA and Sagdeev RZ, J. Photochem. Photobiol. A: Chem, 2004, 162, 371–379.
35. Beeby A, Clarkson IM, Dickins RS, Faulkner S, Parker D, Royle L, de Sousa AS, Gareth Williams JA and Woods M, J. Chem. Soc., Perkin Trans 2, 1999, DOI: 10.1039/A808692C, 493–504.
36. Alpha B, Ballardini R, Balzani V, Lehn J-M, Perathoner S and Sabbatini N, Photochem. Photobiol, 1990, 52, 299–306.
37. D'Aléo A, Picot A, Beeby A, Gareth Williams JA, Le Guennic B, Andraud C and Maury O, Inorg. Chem, 2008, 47, 10258–10268. [PubMed: 18937447]
38. Latva M, Takalo H, Mukkala V-M, Matachescu C, Rodríguez-Ubis JC and Kankare J, J. Lumin, 1997, 75, 149–169.

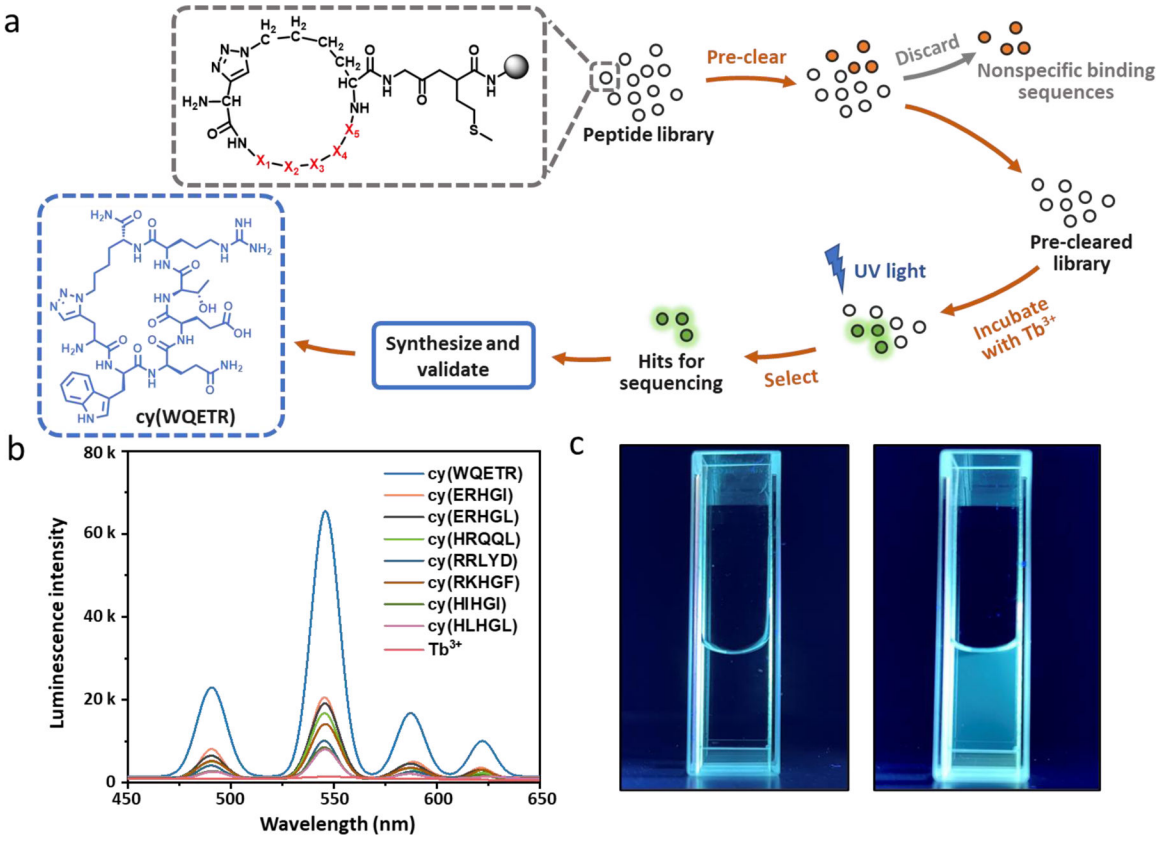

Fig. 1.

(A) Schematic illustration of the peptide library screening strategy and the structure of cy(WQETR). (B) Luminescence emission spectra of Tb^{3+} incubated with various hits. (C) Digital images of 0.5 mM of Tb^{3+} solution (left cuvette) and 0.5 mM of Tb^{3+} incubated with 5 mM of cy(WQETR) (right cuvette) excited with a hand-held UV lamp at 365 nm.

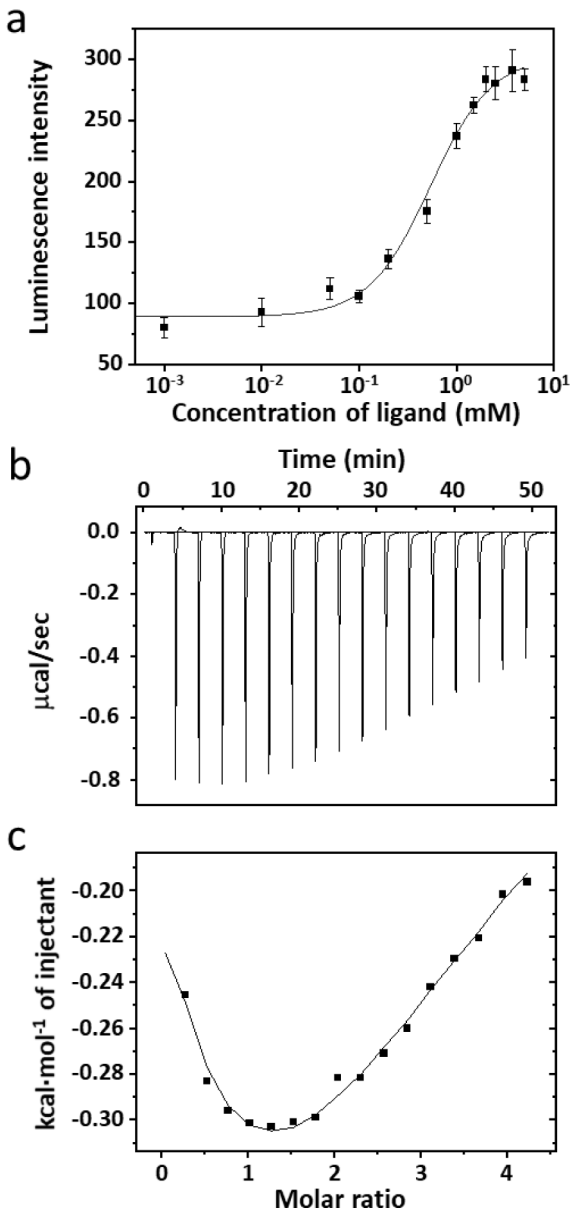

Fig. 2.

(A) Binding affinity of cy(WQETR) to Tb^{3+}. (B) ITC titration raw data for sequential injections of 0.5 mM of cy(WQETR) to Tb^{3+} solution and (C) the heat evolved (kcal) per mole of cy(WQETR) added. The data (filled squares) were fitted with a two sequential-binding sites model, with K_1=750±18 M^{-1}, ΔH_1=−818.4±18.5 cal·mol^{-1}, ΔS_1=10.4 cal·mol^{-1}·K^{-1}; K_2=679±16 M^{-1}, ΔH_2=−1832±38.8 cal·mol^{-1}, ΔS_2=6.81 cal·mol^{-1}·K^{-1}.

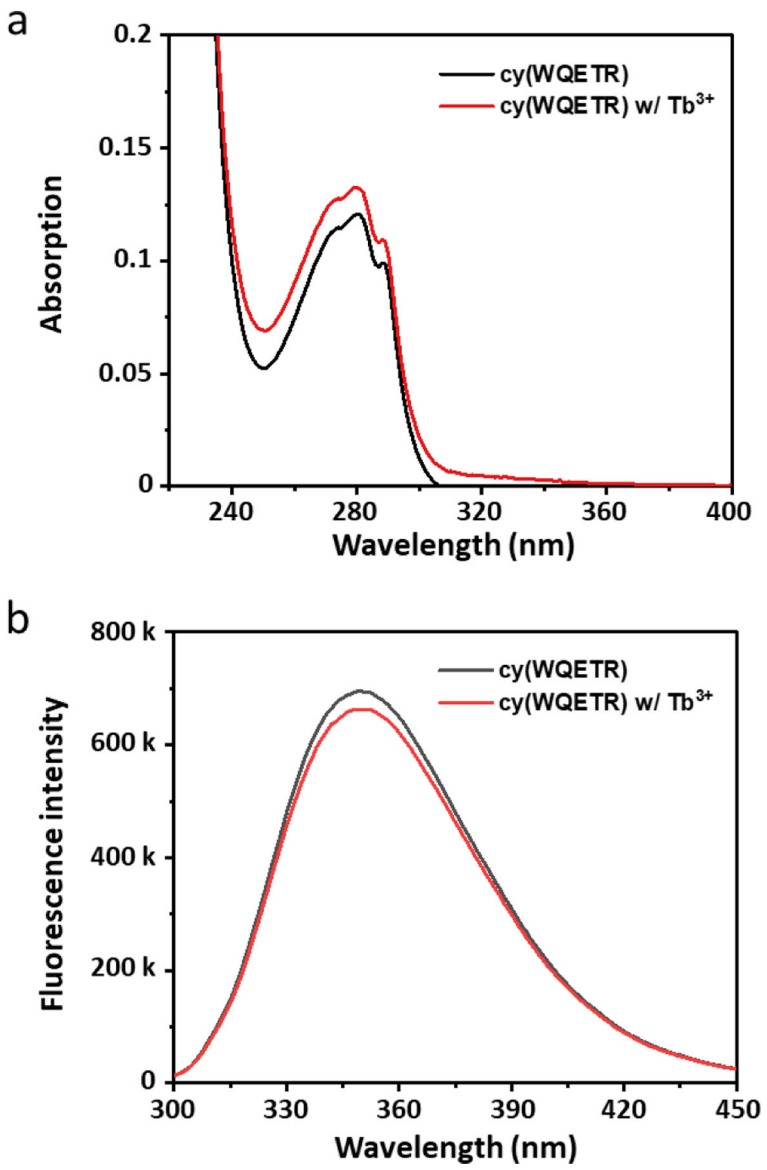

Fig. 3.

(A) UV-vis absorption and (B) Tryptophan fluorescence intensity of 50 μM of cy(WQETR) and 50 μM of cy(WQETR) incubated with 5 μM of Tb^{3+}.

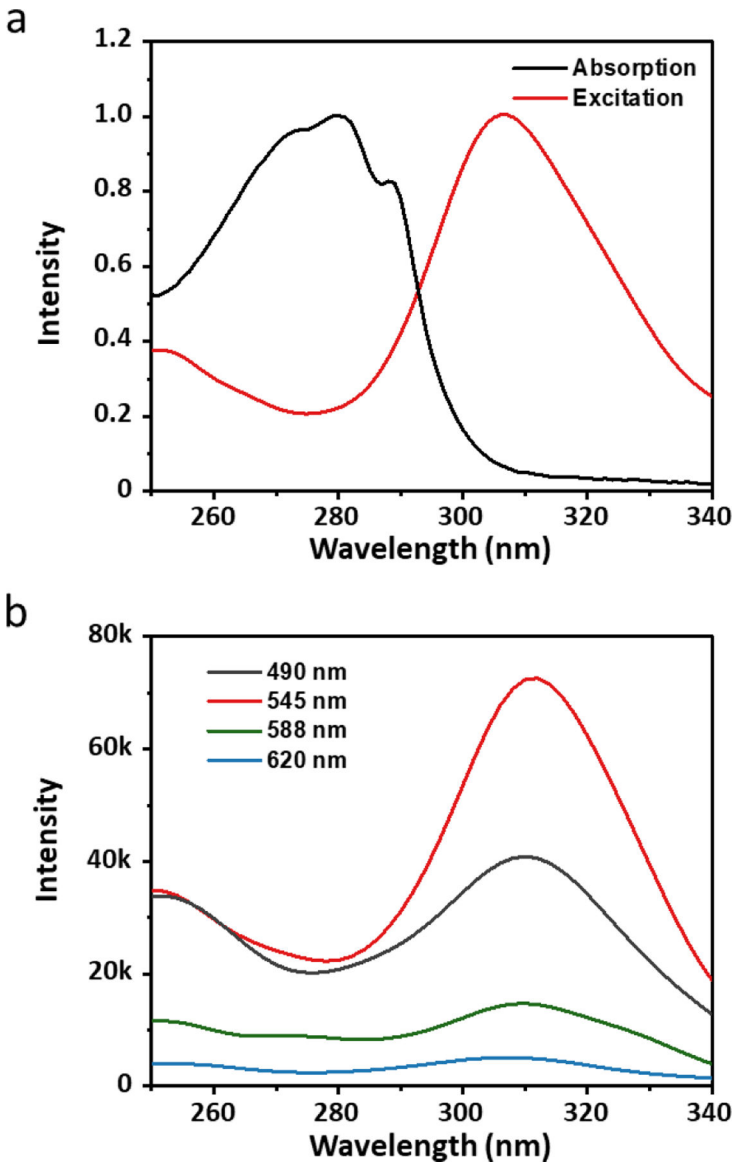

Fig. 4.

(A) Absorption and excitation spectra of the cy(WQETR)-Tb system. (B) Excitation profiles of cy(WQETR)-Tb system corresponding to different emission bands.

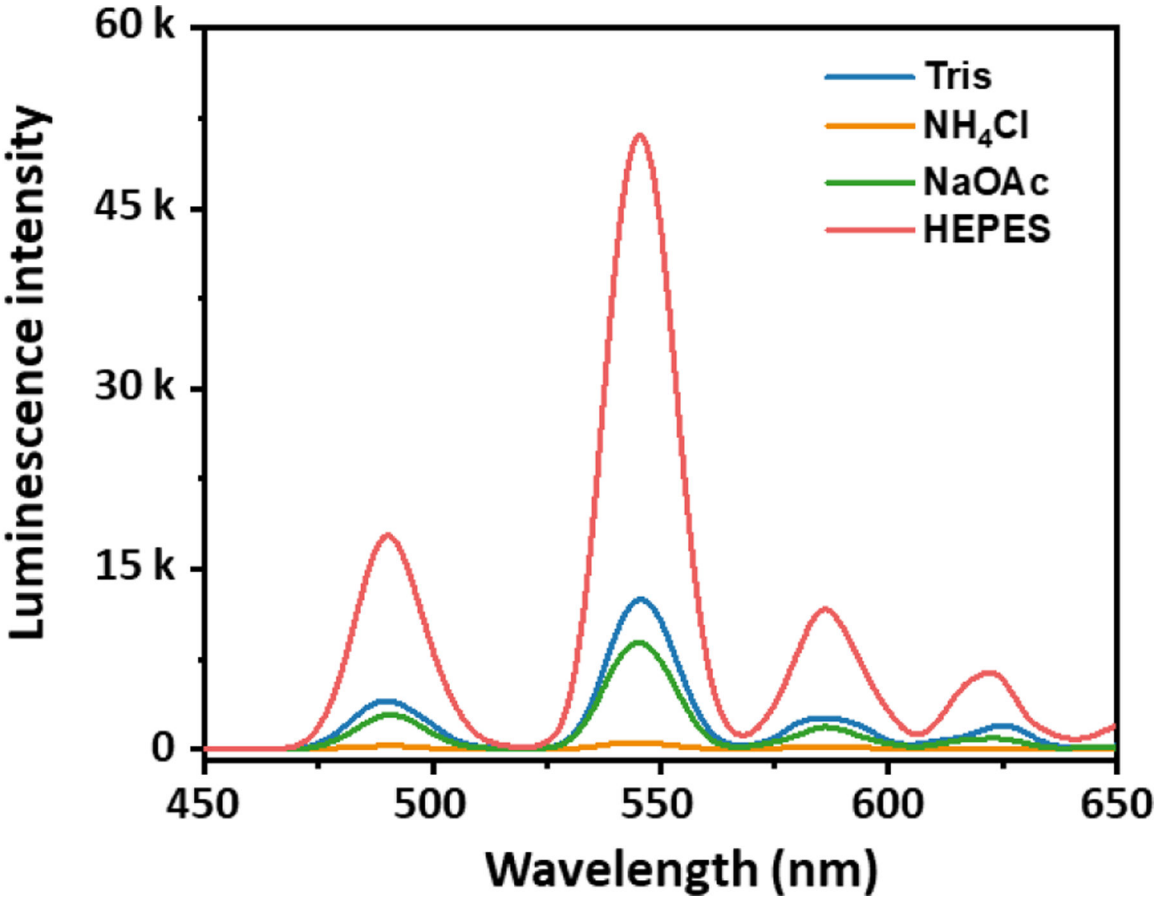

Fig. 5.

Luminescence emission spectra of Tb^{3+} incubated with cy(WQETR) in Tris, NH_4Cl, NaOAc, and HEPES buffer. All buffers had a pH of 7.4.

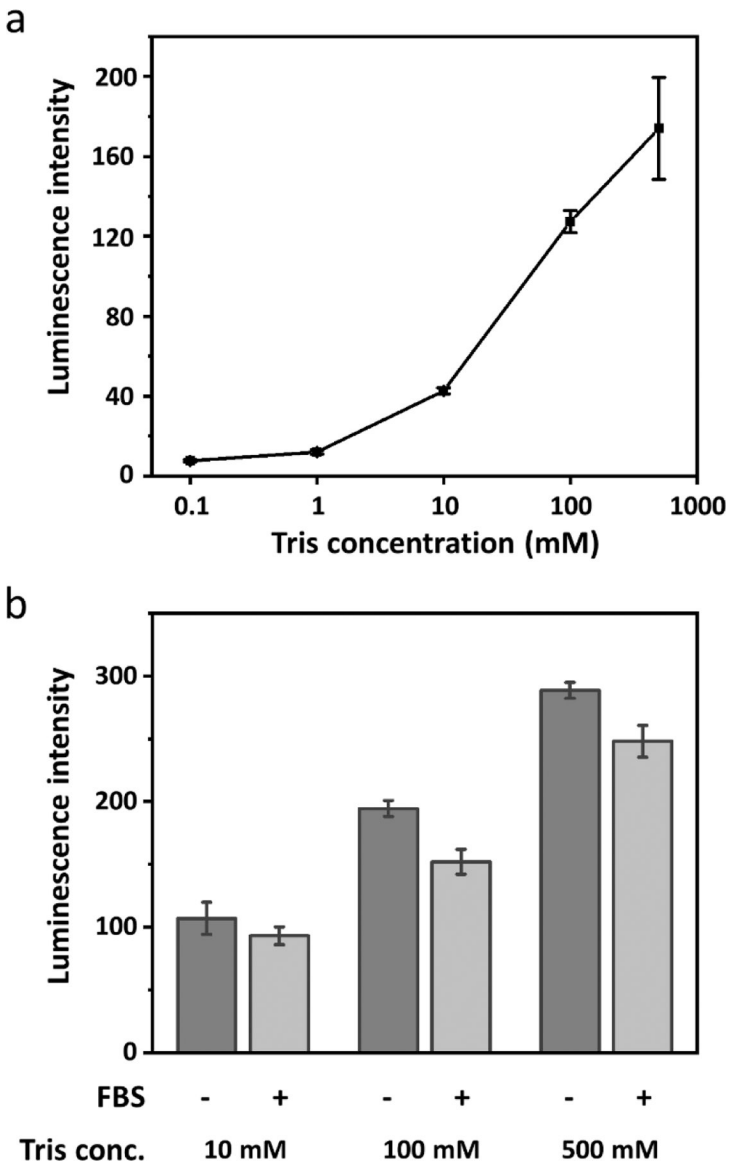

Fig. 6.

Luminescence intensities of 0.5 mM of Tb^{3+} incubated with 5 mM of cy(WQETR) at 545 nm under various concentrations of (A) Tris buffer, and (B) Tris in cell culture media DMEM with or without fetal bovine serum (FBS).